ORGANOMETALLICS
Article
pubs.acs.org/Organometallics

Synthesis and Reactions of a Hybrid Tristibine Ligand

Sophie L. Benjamin, William Levason, and Gillian Reid*

School of Chemistry, University of Southampton, Southampton, U.K. SO17 1BJ

Supporting Information

ABSTRACT: The tripodal tristibine $N(CH_2\text{-}2\text{-}C_6H_4SbMe_2)_3$ (L) has been prepared in high yield and characterized by ^1H and $^{13}C\{^1H\}$ NMR spectroscopy and elemental analysis. A range of reactions with transition-metal acceptors were carried out to probe the coordinative properties of L. The 3/1 M/L complex $[\{FeCp(CO)_2\}_3(L)\text{-}\kappa Sb{:}\kappa Sb'{:}\kappa Sb''][BF_4]_3$ involves tridentate bridging coordination of L to three $CpFe(CO)_2$ fragments. In $[Mn(CO)_3(L)][CF_3SO_3]$ the ligand adopts a tridentate chelating mode via a Sb_3 donor set; treatment of this complex with Me_3NO in MeCN solution gave crystals of $[Mn(CO)_2(L)(MeCN)][CF_3SO_3]$, which lost MeCN in vacuo, probably resulting in coordination of $CF_3SO_3^-$ coordination of the $[CF_3SO_3]^-$ anion. $[M(L)][BF_4]$ (M = Ag, Cu) were also prepared. The reaction of L with CuBr leads to isolation of $[Cu_4Br_4(L)_2]$ in the solid state, which contains a Cu_2Br_4 core with a short central Cu⋯Cu distance, capped with Cu(L) units at each end. The transition-metal complexes of L were characterized by elemental analysis, ESI^+ mass spectrometry, IR spectroscopy, and ^1H, $^{13}C\{^1H\}$, and (where appropriate) ^{55}Mn or ^{63}Cu NMR spectroscopy. Solid-state X-ray structures were determined for $[Mn(CO)_3(L)][CF_3SO_3]$, $[Mn(CO)_2(L)(MeCN)][CF_3SO_3]$, $[Cu_4Br_4(L)_2]$, and $[Cu_3Br_2(L)_2][BF_4]$. In each of these structures the chelating ligand adopts a twisted, propeller-like conformation. NMR spectroscopic analysis suggests that the ligand also adopts this rigid conformation in solution.

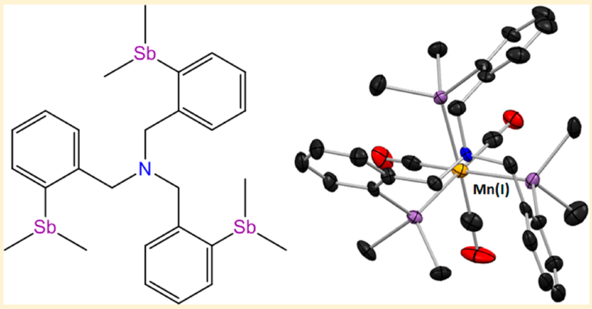

INTRODUCTION

Hybrid stibine ligands, which contain stibine moieties as well as other donor atoms are increasingly of interest. They allow the exploitation of the unusual behaviors which can be accessed using stibine donors within a more stable or strongly binding polydentate framework, and can be adapted for diverse purposes. Very recent examples from Gabbaï and co-workers demonstrate that complexes of the hybrid ligand $Sb\{2\text{-}C_6H_4PPh_2\}_3$ can undergo reaction at the Sb center without decomplexation. Oxidation at Sb by dihalogens leads to the observation of rare "umpolung" type Sb−Au bonds,[1] and a Pd complex of this ligand has been employed for F^- anion sensing by means of reversible acceptance of fluoride ions by the Sb center, which causes measurable changes in the ligand's coordination environment.[2]

The study of intramolecular hypervalent interactions between stibines or bismuthines and lighter heteroatoms has also emerged as a major area of interest in recent years.[3] This phenomenon is not observed in compounds of the lighter group 15 elements such as phosphines; in fact, there is now substantial evidence that heavier group 15 donors support chemistry which is in many cases distinct from that of their lighter counterparts.[4,5] Though this understanding has led to increased research into the synthesis and coordination of organostibines in recent decades, this has been limited almost entirely to monodentate and a smaller number of bidentate examples. Only one tritertiary stibine ligand has been coordinated to transition-metal centers, the tripodal $MeC(CH_2SbPh_2)_3$, which behaves as a tridentate donor toward group 6 tricarbonyl fragments, as evidenced by the crystal structure of $[Mo(CO)_3\{MeC(CH_2SbPh_2)_3\}]$.[6] In early work, the synthesis of the flexible $N(CH_2CH_2CH_2SbR_2)_3$ (R = Me, Ph) was also described, but no complexes were reported.[7]

We have previously reported the synthesis of several hybrid distibine ligands and their complexation to a range of transition-metal centers.[8−11] Here we report the synthesis and some coordination studies of the hybrid tristibine $N(CH_2\text{-}2\text{-}C_6H_4SbMe_2)_3$, a potentially tetradentate ligand and a very rare example of a triorganostibine.

RESULTS AND DISCUSSION

Hybrid tristibine synthesis. The hybrid tristibine ligand $N(CH_2\text{-}2\text{-}C_6H_4SbMe_2)_3$ (**1**) was synthesized as shown in Scheme 1. The precursor $N(CH_2\text{-}2\text{-}C_6H_4Br)_3$ was made via a literature preparation,[12] and the three stibine moieties were introduced in the final step, to minimize the potential for cleavage of the fragile C−Sb bonds. The reaction conditions of this step were critical to the isolation of a pure product. Slow addition of the trilithiate to the flask containing the halostibine and the maintenance of low temperatures throughout allowed the tristibine to be obtained in extremely high yield (82%).

The ligand is an oxygen-sensitive viscous oil; it was stored and used as a stock solution in CH_2Cl_2. ^1H NMR spectroscopy shows two sharp singlets in a 3:1 ratio corresponding to the Me_2Sb and CH_2N groups, respectively, as well as four clearly

Received: March 12, 2013
Published: April 15, 2013

dx.doi.org/10.1021/om400205d | *Organometallics* 2013, 32, 2760−2767

Scheme 1. Synthesis of $N(CH_2\text{-}2\text{-}C_6H_4SbMe_2)_3$

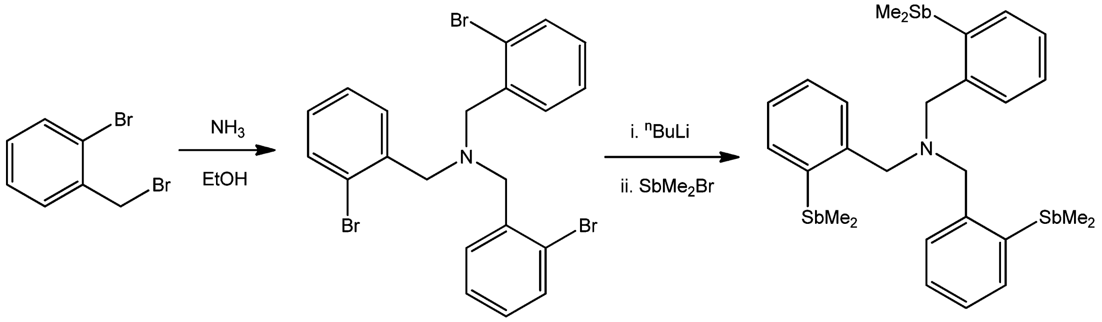

resolved multiplets in the aromatic region. The $^{13}C\{^1H\}$ NMR spectrum has a single MeSb resonance to low frequency of 0 ppm, as is characteristic of alkylstibines, as well as resonances corresponding to CH_2N and six aromatic carbons.

Addition of MeI to a solution of the ligand in MeCN resulted in the precipitation of a white solid. The ESI^+ mass spectrum shows both the doubly and singly methylated products, although no peak was observable for a triply methylated tricationic species.

A number of other routes were investigated for the synthesis of this ligand; the order of addition was found to be a key factor. Addition of the halostibine to the organolithiate, rather than vice versa, resulted in observation of several products, including evidence of the formation of cyclic species. In one case methylation of the product mixture using MeI resulted in isolation of a few crystals of the cyclized stibonium salt $[(Me_2Sb\text{-}2\text{-}C_6H_4CH_2)N(CH_2\text{-}2\text{-}C_6H_4)_2SbMe_2][I]$, which were identified by a single-crystal X-ray structure determination. The structure of the cation (Figure 1) shows a hypervalent interaction between the Sb and N atoms contained in the cyclic moiety (Sb···N = 2.565(4) Å), which is comparable to that seen in uncharged cyclic azastibocines such as $MeN(CH_2\text{-}2\text{-}C_6H_4)_2SbCCPh$ (Sb···N = 2.538(3) Å).[13]

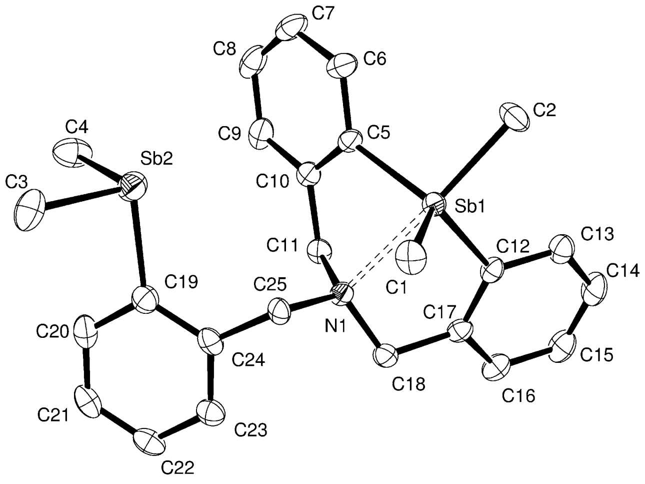

Figure 1. View of the structure of $[(Me_2Sb\text{-}2\text{-}C_6H_4CH_2)N(CH_2\text{-}2\text{-}C_6H_4)_2SbMe_2]^+$ with the atom-numbering scheme. Ellipsoids are drawn at the 50% probability level, and H atoms are omitted for clarity. Selected bond lengths (Å) and angles (deg): Sb1−C5 = 2.109(5), Sb1−C12 = 2.108(5), Sb1−C1 = 2.116(5), Sb1−C2 = 2.134(5), Sb2−C3 = 2.154(6), Sb2−C4 = 2.172(6), Sb2−C19 = 2.188(6), Sb1···N1 = 2.565(4); C5−Sb1−C12 = 115.18(18), C5−Sb1−C1 = 117.6(2), C1−Sb1−C2 = 102.4(2), C1−Sb1···N1 = 87.12(18), C2−Sb1···N1 = 170.41(19), C3−Sb2−C4 = 94.8(3).

In addition to the presence of four donor atoms, the backbone of the ligand **1** has some degree of flexibility. This combination could give rise to a number of different potential coordination modes (Figure 2). These include the very rare Sb_3 chelating mode and the unknown Sb_3N tetradentate chelating mode. The coordination chemistry of this ligand with transition metals was investigated with this versatility in mind, the specific choice of metal centers being designed to probe the possible coordination modes and geometries of the ligand (Scheme 2).

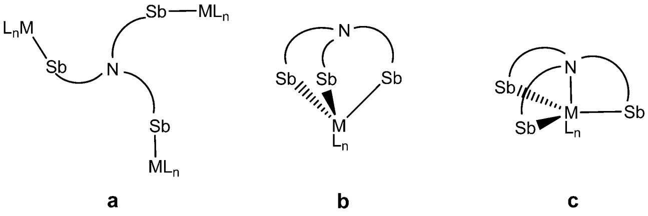

Figure 2. Examples of possible coordination modes of the ligand $N(CH_2\text{-}2\text{-}C_6H_4SbMe_2)_3$: (a) *κSb:κSb′:κSb″*; (b) Sb_3 tridentate chelating; (c) Sb_3N tetradentate chelating.

Transition-Metal Complexes of $N(CH_2\text{-}2\text{-}C_6H_4SbMe_2)_3$.

$[\{FeCp(CO)_2\}_3\{N(CH_2\text{-}2\text{-}C_6H_4SbMe_2)_3\text{-}\kappa Sb{:}\kappa Sb'{:}\kappa Sb''\}][BF_4]_3$ **(2).** The precursor $[FeCp(CO)_2(thf)][BF_4]$ was prepared in situ and provides one easily accessible coordination site via displacement of the labile thf ligand.[14] Reaction of this precursor with $N(CH_2\text{-}2\text{-}C_6H_4SbMe_2)_3$ resulted in formation of the 3/1 complex as an orange solid. The ^1H and $^{13}C\{^1H\}$ NMR spectra were collected in CD_3CN, as the compound was only sparingly soluble in chlorinated solvents, and show one environment for each of the MeSb, CH_2N, and Cp organic moieties. In the $^{13}C\{^1H\}$ NMR spectrum there is a resonance at 210.4 ppm which corresponds to a single metal carbonyl environment. This is supported by both the solution and solid-state IR spectra, which show two strong peaks in the CO region ($a_1 + b_1$), with frequencies almost identical with those of the model complex $[FeCp(CO)_2(SbMe_2Ph)][BF_4]$ (2046, 2002 vs 2046, 2001 cm^{-1}). These observations are consistent with a single environment for the three $CpFe(CO)_2$ fragments, each of which is coordinated to one of the three stibine moieties of the ligand. In related complexes of hybrid stibines and bismuthines hypervalent interactions have been observed, which can cause observable splitting in the solid-state IR spectra due to the resulting inequivalence of the metal centers.[10] There is no evidence for this behavior in the IR spectra of $[\{FeCp(CO)_2\}_3\{N(CH_2\text{-}2\text{-}C_6H_4SbMe_2)_3\}][BF_4]_3$.

Scheme 2. Reactions of $N(CH_2\text{-}2\text{-}C_6H_4SbMe_2)_3$ (L) with Transition-Metal Acceptors

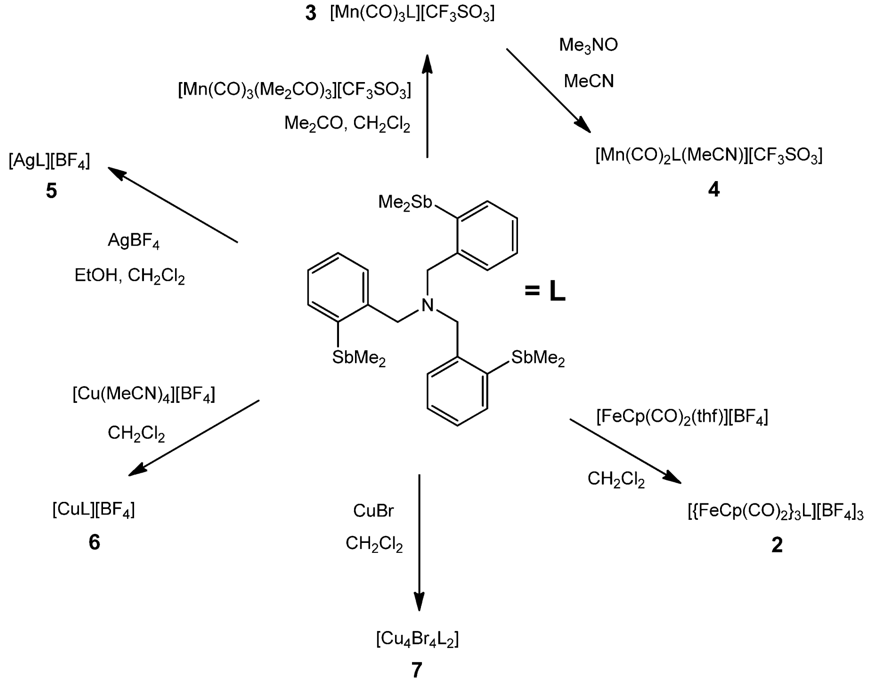

Crystals of the material were grown by several methods, but in each case X-ray crystallographic studies revealed severe disorder within the structure. Though the positions of the heavy atoms could be sufficiently determined to support the assignment of a single ligand bridging three $FeCp(CO)_2$ fragments ($\kappa Sb{:}\kappa Sb'{:}\kappa Sb''$), the disorder of the lighter atoms could not be modeled satisfactorily.

Mn(I) Carbonyl Complexes of $N(CH_2\text{-}2\text{-}C_6H_4SbMe_2)_3$. Manganese(I) carbonyl fragments are soft Lewis acids which are well suited to coordination with stibine ligands, several complexes with distibines being known.[15] They allow the number of vacant sites to be varied in a controllable way, by careful choice of precursor and decarbonylation or halide abstraction from existing complexes.[16] They also provide several spectroscopic probes, making them good candidates for the exploration of the coordination modes of $N(CH_2\text{-}2\text{-}C_6H_4SbMe_2)_3$. Coordination of soft Sb donors to the Mn(I) center is preferred over coordination of amine N donors, though both are observed in $[Mn(CO)_3\{MeN(CH_2\text{-}2\text{-}C_6H_4SbMe_2)_2\}][CF_3SO_3]$, a complex of the corresponding hybrid distibine ligand.[11]

*$[Mn(CO)_3\{N(CH_2\text{-}2\text{-}C_6H_4SbMe_2)_3\}][CF_3SO_3]$ (**3**).* Stirring of $[Mn(CO)_3(OCMe_2)_3][CF_3SO_3]$ with $N(CH_2\text{-}2\text{-}C_6H_4SbMe_2)_3$ in acetone solution resulted in the formation of *fac*-$[Mn(CO)_3\{N(CH_2\text{-}2\text{-}C_6H_4SbMe_2)_3\}][CF_3SO_3]$, isolated after workup as a bright orange powder. The structure was determined by X-ray diffraction and shows the three Sb donors of the ligand facially coordinated to the Mn center, each *trans* to a CO group, with the ligand backbone arranged in a propeller-like conformation (Figure 3). The central tertiary amine is uncoordinated (N···Mn = 4.1637(9) Å) and roughly equidistant from each Sb atom (N···Sb = 3.521(8), 3.601(7), and 3.573(7) Å). These distances are similar to the sum of the van der Waals radii of Sb and N (3.55 Å),[17] meaning no hypervalent interactions are present between the amine and any of the Sb atoms. It is likely that, within the rigid conformation of the ligand arising from tridentate coordination, close approach of N to one or more Sb atoms would be disfavored, as it would introduce too much strain into the ligand backbone. One solvent $CHCl_3$ molecule and one toluene molecule are present in the asymmetric unit, and long contacts (~3.2 Å) are present between two of the CO groups and Cl atoms on the $CHCl_3$ solvate.

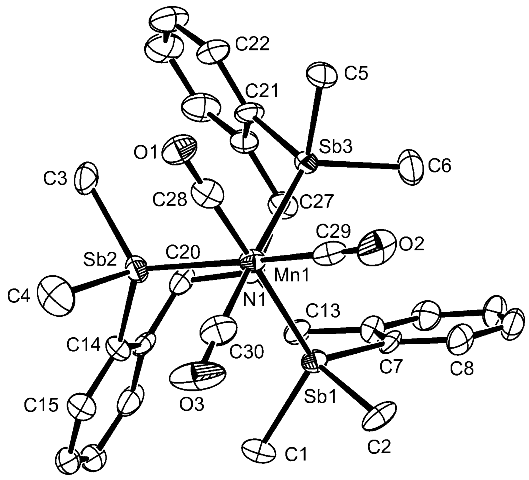

Figure 3. View of the structure of $[Mn(CO)_3\{N(CH_2\text{-}2\text{-}C_6H_4SbMe_2)_3\}]^+$ showing the atom-labeling scheme. Ellipsoids are drawn at the 50% probability level, and H atoms are omitted for clarity. Selected bond lengths (Å) and angles (deg): Sb3−Mn1 = 2.584(2), Sb1−Mn1 = 2.599(2), Sb2−Mn1 = 2.586(2), Mn1−C29 = 1.798(12), Mn1−C28 = 1.800(11), Mn1−C30 = 1.800(12); Sb2−Mn1−Sb1 = 94.84(5), Sb3−Mn1−Sb2 = 95.42(5), Sb3−Mn1−Sb1 = 94.44(5), C29−Mn1−Sb1 = 88.2(3), C28−Mn1−Sb1 = 178.4(3), C30−Mn1−Sb1 = 84.6(3).

The ^1H NMR spectrum shows two peaks of equal integration corresponding to the MeSb protons, and two doublets are observed for the protons of the CH_2N moieties. The $^{13}C\{^1H\}$ NMR spectrum shows two peaks in the MeSb region but only one corresponding to CH_2N. It can be concluded that reversal of the twist in the ligand backbone conformation either is prevented or is slow on the NMR time scale. This results in distinct environments for the two Me groups on each Sb and for the two protons on each benzyl group, the latter then geminally coupling to give rise to the observed doublets.

In the CO region of the $^{13}C\{^1H\}$ NMR spectrum, a broad peak is observed that when closely examined appears to be split into six evenly spaced, overlapping peaks of roughly equal intensity. The intensity of these peaks is modest in comparison to baseline noise, but the observation is reproducible, leading us to postulate that they are the result of $^{55}Mn-^{13}C$ coupling, with a coupling constant of ~154 Hz. $^{55}Mn-^{13}C$ coupling, though not frequently observed, was also reported in the $^{13}C\{^1H\}$ NMR spectrum of *fac*-$[Mn(CO)_3([9]aneS_3)]^+$ with a comparable coupling constant of 160 Hz.[18] The ^{55}Mn NMR ($I = {}^5/_2$, 100%, Ξ = 24.8 MHz, $Q = 0.40 \times 10^{-28}$ m^2)[19] spectrum of this complex contains a very sharp singlet at −1765 ppm, the small line width ($w_{1/2} \approx 85$ Hz) being consistent with a very low electric field gradient at Mn. The shift is comparable with that of *fac*-$[Mn(CO)_3\{MeN(CH_2\text{-}2\text{-}C_6H_4SbMe_2)_2\}][CF_3SO_3]$ (−1745 ppm),[11] the replacement of a stibine donor with a coordinated amine seemingly having only a small effect on the electronic environment of the Mn center; the considerably smaller line width is consistent with the lower electric field gradient in the more symmetrical tristibine complex.

The solution IR spectrum of this complex displays two sharp bands in the carbonyl region (a_1 + e). In the solid state splitting of the e mode into two very close bands is observed, a result of asymmetry arising from either the locking of the ligand backbone or interactions of some CO groups with lattice solvent molecules, as is observed in the crystal structure. The ESI$^+$ mass spectrum shows the molecular ion $[Mn(CO)_3\{N(CH_2\text{-}2\text{-}C_6H_4SbMe_2)_3\}]^+$ and $[Mn(CO)_2\{N(CH_2\text{-}2\text{-}C_6H_4SbMe_2)_3\}]^+$, the result of the loss of one CO group.

$[Mn(CO)_2\{N(CH_2\text{-}2\text{-}C_6H_4SbMe_2)_3\}(MeCN)][CF_3SO_3]$ (4). Treatment of the tricarbonyl complex $[Mn(CO)_3\{N(CH_2\text{-}2\text{-}C_6H_4SbMe_2)_3\}][CF_3SO_3]$ with excess Me_3NO in acetonitrile resulted in the isolation of an orange oil. IR spectroscopy showed two bands in the carbonyl region, to low frequency of those in the tricarbonyl starting material. Recrystallization from CH_2Cl_2 and Et_2O gave orange, needle-shaped crystals which were used in single-crystal diffraction studies. The structure (Figure 4) shows a dicarbonyl species, with the ligand coordinated via the three Sb donors and the final coordination site filled by a MeCN molecule. The N atom in the ligand backbone remains uncoordinated, and the conformation of the ligand is very similar to that observed in the structure of the tricarbonyl species discussed above. The Sb−Mn bond distances *trans* to the CO groups (2.5981(11) and 2.6042(11) Å) are almost identical with those in the tricarbonyl, whereas the Sb−Mn distance *trans* to the MeCN ligand is slightly shorter (Sb1−Mn1 = 2.5472(10) Å).

The crystals were isolated by filtration and dried in vacuo for further analysis. The solid and solution-state IR spectra displayed two bands at frequencies almost identical with those observed for the crude product, but no bands corresponding to MeCN were observed. Neither was there any evidence of MeCN in the ^1H or $^{13}C\{^1H\}$ NMR spectra or the elemental analysis, leading to the conclusion that the coordinated MeCN molecule had been lost when the crystals were subjected to vacuum. This requires the sixth coordination site to be filled by a different donor—we propose that this is either the amine from the ligand backbone or the oxygen of the triflate counterion, both behaviors having been observed in the Mn(I) tricarbonyl system of the hybrid amine/stibine ligand $MeN(CH_2\text{-}2\text{-}C_6H_4SbMe_2)_2$.[11] Given that rearrangement of the ligand conformation in the solid state is unlikely, coordination of $[CF_3SO_3]^-$ seems the more plausible of the two.

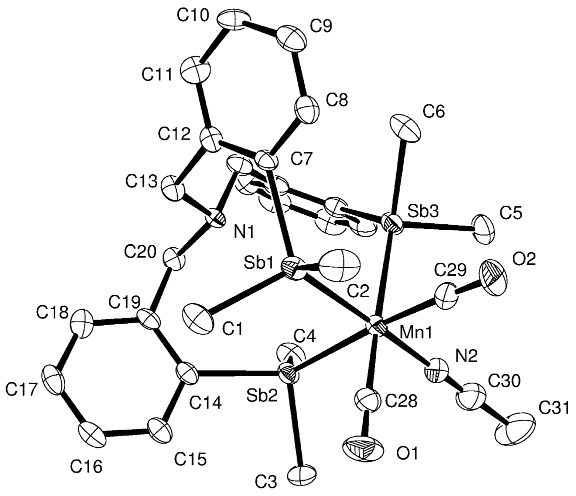

Figure 4. View of the structure of $[Mn(CO)_2\{N(CH_2\text{-}2\text{-}C_6H_4SbMe_2)_3\}(MeCN)]^+$ showing the atom-labeling scheme. Ellipsoids are drawn at the 50% probability level, and H atoms are omitted for clarity. Selected bond lengths (Å) and angles (deg): Sb1−Mn1 = 2.5472(10), Sb2−Mn1 = 2.5981(11), Sb3−Mn1 = 2.6042(11), Mn1−C28 = 1.786(7), Mn1−C29 = 1.792(7), Mn1−N2 = 1.983(6), N2−C30 = 1.132(9); N2−Mn1−Sb1 = 178.04(18), C28−Mn1−N2 = 93.1(3), N2−Mn1−Sb2 = 83.55(18), Sb1−Mn1−Sb2 = 96.59(3), C28−Mn1−Sb1 = 85.0(2).

The ^1H and $^{13}C\{^1H\}$ NMR spectra of this species are both very complex, with a separate environment being observed for each C atom in the molecule. Considering the symmetry of a dicarbonyl complex with one other donor, two of the three ligand arms (those *trans* to the CO groups) would appear to be in the same environment. However, if we consider the ligand backbone to be locked into a twisted position to avoid steric repulsion of the aryl rings, as seen in the crystal structure of the MeCN adduct, the two $Sb_{transCO}$ atoms are then disposed differently from one another relative to MeCN, due to the chirality introduced by the twist in the ligand backbone. This accounts for the three separate environments observed for the three ligand arms. Two very closely spaced peaks are seen in the CO region of the $^{13}C\{^1H\}$ NMR spectrum, indicating that due to the locked ligand conformation the two chemically equivalent carbonyl groups are also in slightly different magnetic environments.

$[Ag\{N(CH_2\text{-}2\text{-}C_6H_4SbMe_2)_3\}][BF_4]$ (5). The reaction of $AgBF_4$ with $N(CH_2\text{-}2\text{-}C_6H_4SbMe_2)_3$ in EtOH followed by washing with Et_2O gave $[Ag\{N(CH_2\text{-}2\text{-}C_6H_4SbMe_2)_3\}][BF_4]$ as a white, mildly light-sensitive powder. The molecular ion, $[Ag\{N(CH_2\text{-}2\text{-}C_6H_4SbMe_2)_3\}]^+$, is the only species observed in the ESI$^+$ mass spectrum. The $^{13}C\{^1H\}$ NMR spectrum reveals two resonances corresponding to MeSb, one corresponding to CH_2N, and six aromatic C atoms. At room temperature the ^1H NMR spectrum is very broad in the methyl and benzyl regions, displaying two broad peaks in each, but upon cooling to −60 °C these resolve into a pair of MeSb singlets and two CH_2N doublets, similar to those seen in the ^1H NMR spectrum of $[Mn(CO)_3\{N(CH_2\text{-}2\text{-}C_6H_4SbMe_2)_3\}][CF_3SO_3]$. This temperature-dependent behavior suggests that at room temperature either the coordination or conformation of the ligand is dynamic on the ^{1}H NMR time scale, whereas at low temperatures the ligand backbone is locked into position with the two MeSb groups and two benzyl protons being inequivalent for each arm of the ligand. Given this information, the ligand could be either tridentate (via the three Sb donors) or tetradentate (with the N atom also coordinated); either would lead to a rigid ligand conformation. Several recrystallizations failed to produce single crystals of quality suitable for X-ray studies.

Cu(I) Complexes of $N(CH_2\text{-}2\text{-}C_6H_4SbMe_2)_3$. Reaction of $[Cu(MeCN)_4][BF_4]$ and $N(CH_2\text{-}2\text{-}C_6H_4SbMe_2)_3$ in CH_2Cl_2 leads to isolation of $[Cu\{N(CH_2\text{-}2\text{-}C_6H_4SbMe_2)_3\}][BF_4]$ (**6**) as a white powder. Solid-state IR spectroscopy confirms the presence of the $[BF_4]^-$ counterion and the absence of any MeCN remaining from the precursor. ESI$^+$ mass spectrometry displays the molecular ion $[Cu\{N(CH_2\text{-}2\text{-}C_6H_4SbMe_2)_3\}]^+$ as the dominant species.

Broad ligand resonances in the ^{1}H NMR spectrum suggest dynamic behavior of the ligand in solution similar to that seen in the silver analogue discussed above. Two environments are observed for each of the MeSb and CH_2N, signifying a locked conformation of the ligand. Broadening could also be due to fast relaxation caused by the proximity of the quadrupolar ^{63}Cu or ^{65}Cu nuclei (^{63}Cu, $I = {}^3/_2$, 69.09%, $\Xi = 26.5$ MHz, $Q = -0.21 \times 10^{-28}$ m^2; ^{65}Cu: $I = {}^3/_2$, 30.91%, $\Xi = 28.4$ MHz, $Q = -0.20 \times 10^{-28}$ m^2),[20] to which we can attribute the broadening in the $^{13}C\{^1H\}$ NMR spectrum of the resonances corresponding to C atoms which are directly bonded to Sb; the *ipso* C atoms are not observed. ^{63}Cu NMR spectroscopy reveals a single, fairly broad resonance at −142 ppm ($w_{1/2} = 3200$ Hz). ^{63}Cu NMR resonances are normally only observed when the metal center is in a high-symmetry environment (giving rise to a small electric field gradient), and for many complexes of Cu(I) with group 15 ligands no such signal is seen.[21] It can be concluded that there is a relatively small electric field gradient around the Cu(I) center in $[Cu\{N(CH_2\text{-}2\text{-}C_6H_4SbMe_2)_3\}][BF_4]$, suggesting a tetrahedral geometry which is often favored by Cu(I) species. Previously structurally characterized complexes of stibine ligands with Cu(I) all feature tetrahedral Cu centers with four Sb donors.[22,23] A tetrahedral geometry would involve tetradentate Sb_3N coordination, though this may be sterically disfavored due to the semirigid nature of the ligand backbone. Other ligands with this backbone architecture, albeit with different donor groups, have been seen to coordinate transition metals in a tetradentate manner, in both distorted-tetrahedral and trigonal-bipyramidal metal geometries, confirming that the backbone does have the required flexibility.[24,25] Despite these considerations, tridentate (Sb_3) coordination cannot be completely ruled out in this case.

Single-crystal X-ray studies would be critical in determining the solid-state structure of this compound. Despite repeated recrystallization attempts, no crystals of suitable quality for X-ray studies could be grown, the compound always being precipitated as a fine powder. One crystallization attempt, involving storage of the reaction mixture at 5 °C over a period of weeks, resulted in the isolation of a few colorless crystals, among which were visible two separate morphologies. X-ray structure determination proved needlelike crystals to be $[Cu_3Br_2\{N(CH_2\text{-}2\text{-}C_6H_4SbMe_2)_3\}_2][BF_4]\cdot 1.5CH_2Cl_2$, whereas block-shaped crystals were $[Cu_4Br_4\{N(CH_2\text{-}2\text{-}C_6H_4SbMe_2)_3\}_2]\cdot 4CH_2Cl_2$. Both of these Cu(I) species were formed as very minor products, with the Br atoms thought to originate from a very small amount of LiBr remaining as an impurity from the ligand preparation. There was no evidence for formation of either of these species in samples of $[Cu\{N(CH_2\text{-}2\text{-}C_6H_4SbMe_2)_3\}][BF_4]$ prepared from a fresh batch of ligand. To allow full characterization, $[Cu_4Br_4\{N(CH_2\text{-}2\text{-}C_6H_4SbMe_2)_3\}_2]$ (**7**) was remade via a direct route as described below.

The structure of $[Cu_3Br_2\{N(CH_2\text{-}2\text{-}C_6H_4SbMe_2)_3\}_2][BF_4]\cdot CH_2Cl_2$ contains a disordered $[BF_4]^-$ anion which was modeled over two positions. The cation is well resolved and contains a centrosymmetric Cu_3Br_2 core, with a center of inversion at Cu2 (Figure 5). The terminal Cu1 is coordinated by one ligand via the three Sb groups, with the Br bridge completing the pseudo-tetrahedral coordination geometry. The propeller type conformation of the ligand is similar to that seen in *fac*-$[Mn(CO)_3\{N(CH_2\text{-}2\text{-}C_6H_4SbMe_2)_3\}][CF_3SO_3]$, though the difference in coordination geometry between the pseudo-tetrahedral Cu and the pseudo-octahedral Mn means the bite angles of the ligands are different (mean ∠Sb−Cu−Sb = 107.2°, ∠Sb−Mn−Sb = 94.9°).

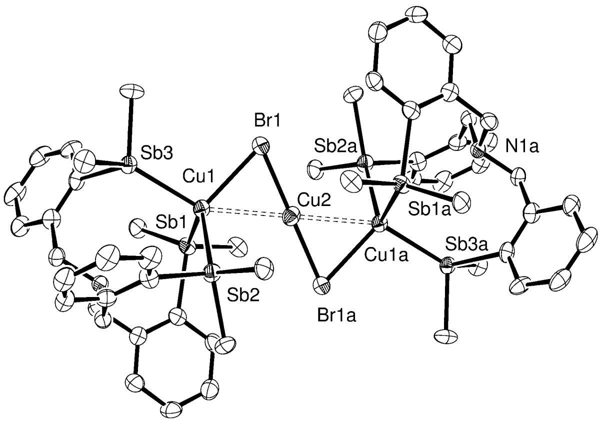

Figure 5. View of the structure of $[Cu_3Br_2\{N(CH_2\text{-}2\text{-}C_6H_4SbMe_2)_3\}_2]^+$ with atom-numbering scheme. Ellipsoids are drawn at the 50% probability level, and H atoms are omitted for clarity. Symmetry operation: (a) $1 - x$, $1 - y$, $1 - z$. Selected bond lengths (Å) and angles (deg): Sb1−Cu1 = 2.5440(14), Sb2−Cu1 = 2.5388(14), Sb3−Cu1 = 2.5378(16), Br1−Cu2 = 2.2665(13), Br1−Cu1 = 2.5373(16), Cu1···Cu2 = 2.6900(17); Cu2−Br1−Cu1 = 67.84(5), Br1−Cu1−Sb3 = 102.73(6), Br1−Cu1−Sb2 = 118.70(5), Br1−Cu1−Sb1 = 113.06(5), Sb2−Cu1−Sb1 = 107.67(6), Br1−Cu1···Cu2 = 51.29(3), Sb1−Cu1···Cu2 = 90.06(3), Br1−Cu2···Cu1 = 60.87(4).

Cu2 is also in the Cu(I) oxidation state but is in a linear coordination environment between the two symmetry-related Br1 atoms. The angle ∠Cu1−Br−Cu2 is very acute (67.84(5)°), meaning Cu1−Cu2 is short (2.690(2) Å), a common phenomenon in polynuclear Cu(I) species. This should not be viewed as a Cu−Cu bond, as Cu(I) has a closed-shell electronic configuration, but could be the result of a type of attractive dispersion interaction which has been termed "cuprophilicity".[26]

The second serendipitously isolated species, $[Cu_4Br_4\{N(CH_2\text{-}2\text{-}C_6H_4SbMe_2)_3\}_2]$, was subsequently prepared directly by stirring of CuBr and $N(CH_2\text{-}2\text{-}C_6H_4SbMe_2)_3$ in a 2/1 ratio in CH_2Cl_2 solution. Crystals of this material with a different unit cell were also analyzed by X-ray diffraction and proved to be the same molecule but without the solvated CH_2Cl_2 molecules (Figure 6). The bond lengths and angles within the complex are very similar between the two structures; the data for the solvated complex are presented in the Supporting Information.

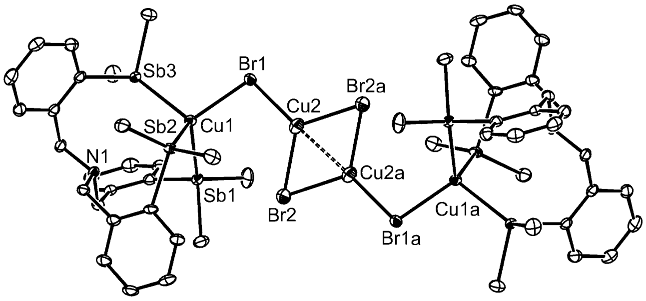

Figure 6. View of the structure of $[Cu_4Br_4\{N(CH_2\text{-}2\text{-}C_6H_4SbMe_2)_3\}_2]$ with atom-numbering scheme. Ellipsoids are drawn at the 50% probability level, and H atoms are omitted for clarity. Symmetry operation: (a) $^1/_2 - x$, $^3/_2 - y$, $1 - z$. Selected bond lengths (Å) and angles (deg): Sb1−Cu1 = 2.5190(8), Sb2−Cu1 = 2.5134(9), Sb3−Cu1 = 2.5300(7), Br1−Cu2 = 2.3419(9), Br1−Cu1 = 2.4253(8), Br2−Cu2 = 2.4027(9), Br2−Cu2a = 2.4297(9), Cu2···Cu2a = 2.5763(12); Cu2−Br1−Cu1 = 99.31(3), Cu2−Br2−Cu2a = 64.43(3), Br1−Cu1−Sb2 = 117.10(3), Br1−Cu1−Sb1 = 110.38(3), Sb2−Cu1−Sb1 = 106.86(3), Br1−Cu1−Sb3 = 105.36(3), Sb2−Cu1−Sb3 = 110.08(3), Sb1−Cu1−Sb3 = 106.64(3), Br1−Cu2−Br2 = 124.06(3), Br1−Cu2−Br2a = 120.33(3), Br2−Cu2−Br2a = 115.57(3), Br1−Cu2···Cu2a = 176.93(4).

The molecule comprises a central Cu_2Br_4 unit with trigonal-planar Cu(I) centers which is structurally comparable with the well-known $[Cu_2Br_4]^{2-}$ anion, though in this case each outer Br atom bridges to a pseudo-tetrahedral $[Cu\{N(CH_2\text{-}2\text{-}C_6H_4SbMe_2)_3\}]^+$ unit, which has a geometry comparable to that of the equivalent moiety in $[Cu_3Br_2\{N(CH_2\text{-}2\text{-}C_6H_4SbMe_2)_3\}_2][BF_4]\cdot CH_2Cl_2$. The central Cu(I)···Cu(I) distance of 2.5763(12) Å is shorter than that in any $[Cu_2Br_4]^{2-}$ unit previously reported in the Cambridge Structural Database.[27]

Similar halocuprate oligomers in which the terminal Cu atoms are coordinated by neutral ligands have been reported. For example, the mixed-valence $[Cu^{II}(4,4'\text{-}Me_2\text{-}2,2'\text{-bipy})_2(\mu\text{-}Br)Cu^{I}(\mu\text{-}Br)_2Cu^{I}Br]$ contains a central Cu_2Br_4 unit geometrically comparable to the core of $[Cu_4Br_4\{N(CH_2\text{-}2\text{-}C_6H_4SbMe_2)_3\}_2]$, though in this case it is only capped at one end.[28] Another mixed-valence species with a very similar geometry is $[Cu^{II}Br(C_{33}H_{43}N_3)]_2[Cu^{I}_2Br_4]$, which, like $[Cu_4Br_4\{N(CH_2\text{-}2\text{-}C_6H_4SbMe_2)_3\}_2]$, is capped at both ends by coordinated Cu moieties, except that the Cu^{II}−Br distance of 2.689(2) Å is long enough for this to be considered as an associated ion pair.[29]

The isolation of finite chains or clusters of halide-bridged Cu(I) atoms within more complex systems is common, and it has been observed that the nature of the cation affects the formation of these anions in the solid state.[30] However, studies have shown that these conformations are not generally retained in solution, extensive dissociation to simple anions generally being observed.[31] It seems probable that the bulky nature of the $[Cu\{N(CH_2\text{-}2\text{-}C_6H_4SbMe_2)_3\}]^+$ moiety is what causes the crystallization of species containing discrete polynuclear Cu(I) bromide cores, but it is likely that these structures are dissociated in solution. The peaks in the ^1H NMR spectrum of $[Cu_4Br_4\{N(CH_2\text{-}2\text{-}C_6H_4SbMe_2)_3\}_2]$ are extremely broad, with two pairs of resonances which can be assigned to MeSb and CH_2N, suggesting that the ligand retains coordination in solution but either the coordination or the conformation of the ligand is dynamic on the ^1H NMR time scale. Peaks are observed in the $^{13}C\{^1H\}$ NMR spectrum for the CH_2N moiety and the six aromatic C atoms, though none could be discerned for MeSb. No signal was observed in the ^{63}Cu NMR spectrum, unsurprisingly considering the likelihood of dissociation in solution leading to more than one low-symmetry ^{63}Cu environment. The main peak in the high-resolution ESI^+ spectrum is $[CuL]^+$ (L = $N(CH_2\text{-}2\text{-}C_6H_4SbMe_2)_3$), but lower intensity peaks can also be observed for aggregates $[Cu_nBr_{n-1}L_2]^+$ (n = 2−5).

■ CONCLUSIONS

A high-yielding synthesis of a very rare tristibine has been reported. Complexes of $N(CH_2\text{-}2\text{-}C_6H_4SbMe_2)_3$ with a variety of transition-metal fragments represent the first coordination complexes of a tetradentate ligand containing Sb donors. Through careful selection of transition-metal acceptors it has been shown that this ligand is capable of coordinating in several different modes, though a marked preference for tridentate chelating Sb_3 donation was observed in the complexes obtained. This could be due to either a thermodynamic preference for tridentate coordination or simply an increased tendency for crystallization of these rigid structures. Examples of this mode have been observed in both octahedral and tetrahedral metal geometries, demonstrating the flexible bite angle of the ligand; in each case the ligand backbone adopts a propeller-like conformation which leads to magnetic inequivalence of chemically equivalent organic moieties. The κSb:$\kappa Sb'$:$\kappa Sb''$ mode was also observed, and there is some evidence to support tetradentate coordination of the ligand in $[Cu\{N(CH_2\text{-}2\text{-}C_6H_4SbMe_2)_3\}][BF_4]$, though this could not be structurally confirmed. The bulky nature of the ligand gives rise to the isolation of unusual copper(I) bromide oligomers in the solid state, which contain short Cu···Cu distances.

■ EXPERIMENTAL SECTION

Infrared spectra were recorded as Nujol mulls between NaCl plates using a Perkin-Elmer Spectrum 100 spectrometer over the range 4000−500 cm^{-1}, and solution spectra used NaCl solution cells over the range 2200−1800 cm^{-1}. ^1H and $^{13}C\{^1H\}$ NMR spectra were recorded using a Bruker AV300 or Bruker DPX400 spectrometer at ambient temperature (25 °C) unless otherwise stated and are referenced to the residual solvent signal. Microanalyses on new complexes were outsourced to Medac Ltd. or London Metropolitan University. Positive ion electrospray (ESI^+) mass spectra were run in MeCN solution using a VG Biotech platform. Preparations were undertaken using standard Schlenk and glovebox techniques under a N_2 atmosphere. Solvents were dried by distillation from CaH_2 (CH_2Cl_2, MeCN), Na/benzophenone ketyl (thf, diethyl ether), Na wire (toluene, hexane), or Mg/I_2 (EtOH). Starting materials were purchased from Sigma Aldrich and used as received. $SbMe_2Ph$ was made as described previously.[32]

$N(CH_2\text{-}2\text{-}C_6H_4SbMe_2)_3$ (1). A solution of $SbMe_2Ph$ (3.73 g, 16.3 mmol) in toluene (300 mL) was flushed with HBr gas for 15 min. The resulting $SbMe_2Br$ solution was stirred under a sealed atmosphere for 30 min, followed by purging with a stream of N_2 gas for 20 h, and then cooled to 0 °C. A thf (250 mL) solution of $N(CH_2\text{-}2\text{-}C_6H_4Br)_3$ (2.67 g, 5.1 mmol) was cooled to −78 °C and ^nBuLi (1.6 M in hexane, 9.56 mL, 15.3 mmol) added dropwise. The resulting pink solution was stirred for 10 min and then added slowly to the cooled, stirred solution of $SbMe_2Br$. The reaction mixture was stirred for 18 h and then degassed and deionized water (100 mL) was added slowly. The organic layer was separated, the aqueous layer was washed with Et_2O

(40 mL), the combined organics were dried over $MgSO_4$ and filtered, and the volatiles were removed in vacuo to give a sticky, opaque white oil. This crude product was redissolved in CH_2Cl_2, the solution was filtered through Celite to remove a small amount of insoluble white powder, and the volatiles were removed in vacuo, yielding a sticky clear oil. Yield: 3.11 g, 82%. Anal. Calcd for $C_{27}H_{36}N_1Sb_3$ (739.5): C, 43.8; H, 4.9; N, 1.9. Found: C, 44.0; H, 4.8; N, 2.0. ^1H NMR ($CDCl_3$): δ 0.89 (s, [18H], MeSb), 3.80 (s, [6H], CH_2N), 7.21 (dt, [3H]), 7.30 (dt, [3H]), 7.48 (dd, [3H]) and 7.62 (dd, [3H]) (aromatic CH). $^{13}C\{^1H\}$ NMR ($CDCl_3$): δ −1.6 (MeSb), 60.5 (CH_2N), 127.2, 128.2, 129.3, 133.4, 138.5, and 144.4 ($C_{aromatic}$).

A small portion of the product was dissolved in MeCN and treated with an excess of MeI, and the mixture was stirred for 5 h. The volatiles were then removed in vacuo, leaving a white solid residue. MS (ESI^+): *m/z* 754 $[N(CH_2\text{-}2\text{-}C_6H_4SbMe_2)_2(CH_2\text{-}2\text{-}C_6H_4SbMe_3)]^+$, 604 $[N(CH_2C_6H_5)(CH_2\text{-}2\text{-}C_6H_4SbMe_2)(CH_2\text{-}2\text{-}C_6H_4SbMe_3)]^+$, 588 $[(Me_2Sb\text{-}2\text{-}C_6H_4CH_2)N(CH_2\text{-}2\text{-}C_6H_4)_2SbMe_2]^+$, 452 $[N(CH_2C_6H_5)_2(CH_2\text{-}2\text{-}C_6H_4SbMe_3)]^+$, 436 $[(C_6H_5CH_2)N(CH_2\text{-}2\text{-}C_6H_4)_2SbMe_2]^+$, 420 $[N(CH_2\text{-}2\text{-}C_6H_4)_3SbMe]^+$, 384.5 $[N(CH_2\text{-}2\text{-}C_6H_4SbMe_2)(CH_2\text{-}2\text{-}C_6H_4SbMe_3)_2]^{2+}$, 309.5 $[N(CH_2C_6H_5)(CH_2\text{-}2\text{-}C_6H_4SbMe_3)_2]^{2+}$, 301.5 $[(Me_3Sb\text{-}2\text{-}C_6H_4CH_2)N(CH_2\text{-}2\text{-}C_6H_4)_2SbMe_2]^{2+}$.

$[\{FeCp(CO)_2\}_3\{N(CH_2\text{-}2\text{-}C_6H_4SbMe_2)_3\}][BF_4]_3$ (2). $[FeCp(CO)_2I]$ (0.25 g, 0.81 mmol) and $Ag[BF_4]$ (0.16 g, 0.81 mmol) were dissolved in CH_2Cl_2 (20 mL), and thf (0.1 mL) was added. The mixture was stirred in the absence of light for 2 h and then filtered to remove the resultant pale precipitate. The red filtrate was added to a solution of $N(CH_2\text{-}2\text{-}C_6H_4SbMe_2)_3$ (0.20 g, 0.27 mmol) in CH_2Cl_2 (5 mL), and the reaction mixture was stirred for 18 h, resulting in an orange solution. The volatiles were removed in vacuo, yielding an orange solid, which was washed with Et_2O (10 mL) and dried in vacuo. Yield: 0.22 g, 53%. Anal. Calcd for $C_{48}H_{51}B_3F_{12}Fe_3NO_6Sb_3$ (1532.2): C, 37.7; H, 3.4; N, 0.9. Found: C, 37.2; H, 2.8; N, 1.0. IR (Nujol/cm^{-1}): 2038 s, br, 1987 s, br (CO), 1049 s, vbr (BF_4). IR (CH_2Cl_2/cm^{-1}): 2046 s, 2001 s. ^1H NMR (CD_3CN): δ 1.76 (s, [18H], MeSb), 3.93 (s, [6H], CH_2N), 5.26 (s, [15H], Cp), 7.41 (m, [3H]), 7.47 (m, [3H]), 7.57 (t, [3H]), 8.05 (d, [3H]), (aromatic CH). $^{13}C\{^1H\}$ NMR (CD_3CN): δ 2.6 (MeSb), 59.0 (CH_2N), 86.7 (Cp), 128.5, 128.8, 129.3, 132.9, 144.5 ($C_{aromatic}$), 210.4 (CO). (ESI^+): *m/z* 547 $[\{FeCp(CO)_2\}_2\{N(CH_2\text{-}2\text{-}C_6H_4SbMe_2)_3\}]^{2+}$, 678 $[\{FeCp(CO)_2\}_3\{N(CH_2\text{-}2\text{-}C_6H_4SbMe_2)_3\}\{BF_4\}]^{2+}$, 860 $[Fe(CO)_2\{N(CH_2\text{-}2\text{-}C_6H_4SbMe_2)_3\}]^+$.

$[Mn(CO)_3\{N(CH_2\text{-}2\text{-}C_6H_4SbMe_2)_3\}][CF_3SO_3]$ (3). A mixture of $[Mn(CO)_5Br]$ (0.074 g, 0.27 mmol) and $Ag[CF_3SO_3]$ (0.069 g, 0.27 mmol) was refluxed for 1 $^1/_2$ h in acetone solution (30 mL). The resultant yellow solution was filtered to remove the off-white precipitate, and a solution of $N(CH_2\text{-}2\text{-}C_6H_4SbMe_2)_3$ (0.20 g, 0.27 mmol) in CH_2Cl_2 (5 mL) was added. The reaction mixture was stirred for 18 h, resulting in a clear orange solution. The volatile components were removed in vacuo, resulting in a bright orange oil. Trituration with Et_2O (15 mL) gave a bright orange solid, which was isolated by filtration. Yield: 0.135 g, 49%. Recrystallization from toluene/$CHCl_3$ (18 °C, 72 h) gave orange-yellow crystals which were used for the X-ray data collection. Anal. Calcd for $C_{31}H_{36}F_3MnNO_6SSb_3$ (1027.9): C, 36.2; H, 3.5; N, 1.4. Found: C, 36.4; H, 4.3; N, 1.5. IR (Nujol/cm^{-1}): 2006 s, 1934 sh, 1926 s (CO), 1262 s, br (CF_3SO_3). IR (CH_2Cl_2/cm^{-1}): 2015 s, 1943 m (CO). ^1H NMR (CD_2Cl_2): δ 0.51 (s, [9H], MeSb), 1.56 (s, [9H], MeSb), 3.05 (d, [3H], CH_2N), 3.80 (d, [3H], CH_2N), 7.4−7.8 (m, [12H], aromatic CH). $^{13}C\{^1H\}$ NMR ($CDCl_3$): δ 0.0 and 1.5 (SbMe), 63.1 (CH_2N), 130.2, 131.8, 132.1, 134.4, 134.7, and 143.1 ($C_{aromatic}$), 218.9 (1:1:1:1:1:1 sextet, $^1J_{MnC} \approx 154$ Hz). ^{55}Mn NMR (CH_2Cl_2/$CDCl_3$): δ −1765 ($w_{1/2}$ = 85 Hz). (ESI^+): *m/z* 878 $[Mn(CO)_3\{N(CH_2\text{-}2\text{-}C_6H_4SbMe_2)_3\}]^+$, 850 $[Mn(CO)_2\{N(CH_2\text{-}2\text{-}C_6H_4SbMe_2)_3\}]^+$.

$[Mn(CO)_2\{N(CH_2\text{-}2\text{-}C_6H_4SbMe_2)_3\}][CF_3SO_3]$ (4). Freshly prepared $[Mn(CO)_3\{N(CH_2\text{-}2\text{-}C_6H_4SbMe_2)_3\}][CF_3SO_3]$ (0.21 g, 0.20 mmol) was dissolved in MeCN (10 mL) and a solution of Me_3NO (0.030 g, 0.40 mmol) in MeCN (10 mL) added. The reaction mixture was stirred for 18 h, and then the volatiles were removed in vacuo, leaving a bright orange oil, which was redissolved in CH_2Cl_2 (10 mL). Et_2O (5 mL) was added, the solution was filtered to remove a small amount of pale solid, and the filtrate was stored at 5 °C over 24 h, yielding orange needlelike crystals and some pale orange solid. The crystals were isolated by decanting the supernatant and their structure was determined by X-ray methods. They were then dried in vacuo for 2 h, after which NMR, IR and elemental analysis was undertaken. Yield: 0.05 g, 25%. Anal. Calcd for $C_{30}H_{36}F_3MnNO_5SSb_3$ (999.4): C, 36.0; H, 3.6; N, 1.4. Found: C, 35.9; H, 3.5; N, 1.6. IR (Nujol/cm^{-1}): 1943 s, 1887 s (CO), 1261 s, br (CF_3SO_3). IR (CH_2Cl_2/cm^{-1}): 1949 s, 1890 s. ^1H NMR ($CDCl_3$): δ 0.26 (s, [3H]), 0.52 (s, [3H]), 0.56 (s, [3H]), 1.22 (s, [3H]), 1.45 (s, [3H]), 1.47 (s, [3H]) (MeSb), 2.82−2.89 (3 overlaid doublets, [3H]), 3.76 (d, $^2J_{HH}$ = 12 Hz, [1H]), 3.83 (d, $^2J_{HH}$ = 12 Hz, [1H]), 3.95 (d, $^2J_{HH}$ = 12 Hz, [1H]) (CH_2N), 7.32−7.45 (m, [8H]), 7.60−7.66 (m, [3H]), 7.82−7.85 (m, [1H]) (aromatic CH). $^{13}C\{^1H\}$ NMR ($CDCl_3$): δ −2.5, −1.5, −1.0, −0.9, −0.3, and 1.6 (MeSb), 63.07, 63.11, and 63.4 (CH_2N), 129.0, 129.2, 130.4, 130.5, 130.6, 132.75, 132.81, 133.0, 133.4, 134.0, 134.1, 134.55, 134.57, 136.2, 136.4, 141.5, 142.6, and 142.8 ($C_{aromatic}$), 223.5 and 223.7 (CO). ^{19}F NMR ($CDCl_3$): δ −78.1. ^{55}Mn NMR (CH_2Cl_2/$CDCl_3$): not observed. (ESI^+): *m/z* 850 $[Mn(CO)_2\{N(CH_2\text{-}2\text{-}C_6H_4SbMe_2)_3\}]^+$.

$[Ag\{N(CH_2\text{-}2\text{-}C_6H_4SbMe_2)_3\}][BF_4]$ (5). $AgBF_4$ (0.053 g, 0.27 mmol) was dissolved in EtOH (20 mL), and a solution of $N(CH_2\text{-}2\text{-}C_6H_4SbMe_2)_3$ (0.20 g, 0.27 mmol) in CH_2Cl_2 (5 mL) was added. The mixture was stirred in the absence of light for 1 $^1/_2$ h, resulting in a slightly cloudy colorless solution, which was filtered, and the volatile components of the filtrate were removed in vacuo. The resultant tacky white solid was washed with Et_2O (20 mL), leaving a fine white powder, which was dried in vacuo for 2 h. Despite drying, both the NMR spectra and the elemental analysis suggested the presence of a less than stoichiometric amount of Et_2O remaining. The NMR resonances correspond exactly to free Et_2O, making it unlikely that this solvent is coordinated to the metal center. Yield: 0.16 g, 61%. Anal. Calcd for $C_{27}H_{36}AgBF_4NSb_3\cdot 0.5C_4H_{10}O$ (971.4): C, 35.8; H, 4.3; N, 1.4. Found: C, 36.8; H, 4.1; N, 1.7. IR (Nujol/cm^{-1}): 1051 vbr (BF_4). ^1H NMR ($CDCl_3$, 25 °C): δ 0.42 (vbr, [9H], MeSb), 1.35 (vbr, [9H], MeSb), 3.09 (vbr, [3H], CH_2N), 3.90 (vbr, [3H], CH_2N), 7.35−7.38 (m, [9H], aromatic CH), 7.49−7.52 (m, [3H], aromatic CH). ^1H NMR ($CDCl_3$, −60 °C): δ 0.32 (s, [9H], MeSb), 1.21 (t, [1.5H], Et_2O) 1.36 (s, [9H], MeSb), 3.08 (d, [3H], CH_2N), 3.47 (q, [1H], Et_2O), 3.87 (d, [3H], CH_2N), 7.35−7.38 (m, [9H], aromatic CH), 7.43−7.46 (m, [3H], aromatic CH). $^{13}C\{^1H\}$ NMR ($CDCl_3$, 25 °C): δ −2.9 (MeSb), 63.2 (CH_2N), 128.8, 129.2, 133.3, 134.0, 135.9, and 141.1 ($C_{aromatic}$). (ESI^+): *m/z* 848 $[Ag\{N(CH_2\text{-}2\text{-}C_6H_4SbMe_2)_3\}]^+$.

$[Cu\{N(CH_2\text{-}2\text{-}C_6H_4SbMe_2)_3\}][BF_4]$ (6). $[Cu(MeCN)_4][BF_4]$ (0.063 g, 0.20 mmol) was dissolved in CH_2Cl_2 (20 mL), and a solution of $N(CH_2\text{-}2\text{-}C_6H_4SbMe_2)_3$ (0.15 g, 0.20 mmol) in CH_2Cl_2 (10 mL) was added. The reaction mixture was stirred for 18 h, resulting in a cloudy, colorless solution, which was filtered and then reduced in vacuo to ∼5 mL. Et_2O (15 mL) was added, precipitating a white solid, which was isolated by filtration and washed with Et_2O (5 mL). Yield: 0.09 g, 50%. Anal. Calcd for $C_{27}H_{36}BCuF_4NSb_3$ (890.1): C, 36.4; H, 4.1; N, 1.6. Found: C, 37.4; H, 4.3; N, 1.5%. IR (Nujol/cm^{-1}): 1057 vbr (BF_4). ^1H NMR ($CDCl_3$): δ 0.47 (br, [9H], MeSb), 1.34 (br, [9H], MeSb), 3.34 (vbr, [3H], CH_2N), 3.86 (vbr, [3H], CH_2N), 7.35−7.52 (m, [12H], CH aromatics). $^{13}C\{^1H\}$ NMR ($CDCl_3$): δ −3.0 (MeSb), 64.6 (CH_2N), 129.1, 129.5, 133.1, 133.9, 134.1, and 140.8 ($C_{aromatic}$). ^{63}Cu NMR ($CDCl_3$): δ −142 ($w_{1/2}$ = 3200 Hz). MS (ESI^+): *m/z* 804 $[Cu\{N(CH_2\text{-}2\text{-}C_6H_4SbMe_2)_3\}]^+$.

$[Cu_4Br_4\{N(CH_2\text{-}2\text{-}C_6H_4SbMe_2)_3\}_2]$ (7). CuBr (0.058 g, 0.40 mmol) was suspended in CH_2Cl_2 (20 mL), and a solution of $N(CH_2\text{-}2\text{-}C_6H_4SbMe_2)_3$ (0.15 g, 0.20 mmol) in CH_2Cl_2 (10 mL) was added. The mixture was stirred for 18 h, and the resultant slightly cloudy, colorless solution was filtered. The filtrate was reduced in volume to ∼5 mL, and Et_2O (15 mL) was added, precipitating a flocculant white solid which was isolated by filtration and washed with Et_2O (5 mL). Yield: 0.12 g, 58%. Colorless block-shaped crystals grew from the filtrate over 2 days, which were used for X-ray data collection. Anal. Calcd for $C_{27}H_{36}Br_2Cu_2N_1Sb_3$ (1026.4): C, 31.6; H, 3.5; N, 1.4. Found: C, 31.9; H, 3.2; N, 1.7. ^1H NMR ($CDCl_3$): δ 0.33 (vbr, [9H], SbMe), 1.17 (vbr, [9H], SbMe), 3.03 (vbr, [3H], CH_2N), 3.81 (vbr,

[3H], CH_2N), 7.28–7.36 (m, [9H], aromatic CH), 7.52–7.54 (m, [3H], aromatic CH). $^{13}C\{^1H\}$ NMR (CD_2Cl_2): δ 63.4 (CH_2N), 129.0, 129.5, 134.0, 134.7, 136.7, and 142.8 ($C_{aromatic}$). MS (HR ESI$^+$): *m/z* 2116 $[Cu_5Br_4\{N(CH_2\text{-}2\text{-}C_6H_4SbMe_2)_3\}_2]^+$, 1972 $[Cu_4Br_3\{N(CH_2\text{-}2\text{-}C_6H_4SbMe_2)_3\}_2]^+$, 1829 $[Cu_3Br_2\{N(CH_2\text{-}2\text{-}C_6H_4SbMe_2)_3\}_2]^+$, 1687 $[Cu_2Br_1\{N(CH_2\text{-}2\text{-}C_6H_4SbMe_2)_3\}_2]^+$, 804 $[Cu\{N(CH_2\text{-}2\text{-}C_6H_4SbMe_2)_3\}]^+$.

X-ray Crystallography. Crystals were obtained as described above. Details of the crystallographic data collection and refinement parameters are given in Table S1 (Supporting Information). Data collection was carried out using either a Rigaku AFC12 goniometer equipped with an enhanced sensitivity (HG) Saturn724+ detector mounted at the window of an FR-E+ SuperBright molybdenum rotating anode generator with VHF Varimax optics (70 μm focus) or a Rigaku R-Axis Spider including curved Fujifilm image plate and a graphite-monochromated sealed-tube Mo generator. Structure solution and refinement were routine[33,34] except where mentioned below; hydrogen atoms on C were added to the model in calculated postions using the default C−H distance. Disorder of the $[BF_4]^-$ unit in $[Cu_3Br_2\{N(CH_2\text{-}2\text{-}C_6H_4SbMe_2)_3\}_2][BF_4]\cdot 1.5CHCl_2$ was modeled over two positions. The site occupation factor for the CH_2Cl_2 solvate molecules was determined by refinement. The toluene solvate in $[Mn(CO)_3\{N(CH_2\text{-}2\text{-}C_6H_4SbMe_2)_3\}][CF_3SO_3]\cdot CHCl_3\cdot C_7H_8$ exhibits disorder which could not be satisfactorily modeled; however, the other components of the structure are well resolved.

The CCDC reference numbers 924062−924067 contain supplementary crystallographic data for this paper. These data can be obtained free of charge from The Cambridge Crystallographic Data Centre via www.ccdc.cam.ac.uk/data_request/cif.

■ ASSOCIATED CONTENT

Ⓢ Supporting Information

CIF files for the crystal structures described, together with crystallographic data (Table S1) and the structural information for $[Cu_4Br_4\{N(CH_2\text{-}2\text{-}C_6H_4SbMe_2)_3\}_2]\cdot 4CH_2Cl_2$. This material is available free of charge via the Internet at http://pubs.acs.org.

■ AUTHOR INFORMATION

Corresponding Author

*E-mail for G.R.: G.Reid@soton.ac.uk.

Notes

The authors declare no competing financial interest.

■ ACKNOWLEDGMENTS

We thank the EPSRC for financial support and for a Doctoral Prize (S.L.B.). We also thank Dr. M. Webster for assistance with crystallographic analyses.

■ REFERENCES

(1) Wade, C. R.; Gabbaï, F. P. *Angew. Chem., Int. Ed.* **2011**, *50*, 7369.

(2) Wade, C. R.; Ke, I.-S.; Gabbaï, F. P. *Angew. Chem., Int. Ed.* **2012**, *51*, 478.

(3) Raţ, C. I.; Silvestru, C.; Breunig, H. J. *Coord. Chem. Rev.* **2013**, *257*, 818.

(4) Levason, W.; Reid, G. *Coord. Chem. Rev.* **2006**, *250*, 2565.

(5) Werner, H. *Angew. Chem., Int. Ed.* **2004**, *43*, 938.

(6) Chiffey, A. F.; Evans, J.; Levason, W.; Webster, M. *Organometallics* **1996**, *15*, 1280.

(7) Levason, W.; Sheikh, B. *J. Organomet. Chem.* **1981**, *209*, 161.

(8) Jura, M.; Levason, W.; Reid, G.; Webster, M. *Dalton Trans.* **2009**, 7811.

(9) Davis, M. F.; Jura, M.; Levason, W.; Reid, G.; Webster, M. *J. Organomet. Chem.* **2007**, *692*, 5589.

(10) Benjamin, S. L.; Karagiannidis, L.; Levason, W.; Reid, G.; Rogers, M. C. *Organometallics* **2011**, *30*, 895.

(11) Benjamin, S. L.; Levason, W.; Reid, G.; Rogers, M. C. *Dalton Trans.* **2011**, *40*, 6565.

(12) Chen, Q.; Buss, C. E.; Young, V. G.; Fox, S. *J. Chem. Crystallogr.* **2005**, *35*, 177.

(13) Kakusawa, N.; Tobiyasu, Y.; Yasuike, S.; Yamaguchi, K.; Seki, H.; Kurita, J. *J. Organomet. Chem.* **2006**, *691*, 2953.

(14) Reger, D. L.; Coleman, C. *J. Organomet. Chem.* **1977**, *131*, 153.

(15) Pope, S. J. A.; Reid, G. *J. Chem. Soc., Dalton Trans.* **1999**, 1615.

(16) Patel, B.; Reid, G. *J. Chem. Soc., Dalton Trans.* **2000**, 1303.

(17) www.ccdc.cam.ac.uk/products/csd/radii/

(18) Connolly, J.; Genge, A. R. J.; Levason, W.; Orchard, S. D.; Pope, S. J. A.; Reid, G. *J. Chem. Soc., Dalton Trans.* **1999**, 2343.

(19) Mason, J. *Multinuclear NMR*; Plenum Press: New York, 1987.

(20) Granger, P. In *Transition Metal Nuclear Magnetic Resonance*; Pregosin, P. S., Ed.; Elsevier: Amsterdam, 1991; p 264.

(21) Black, J. R.; Levason, W.; Spicer, M. D.; Webster, M. *J. Chem. Soc., Dalton Trans.* **1993**, 3129.

(22) Bowmaker, G. A.; Effendy; Hart, R. D.; Kildea, J. D.; de Silva, E. N.; Skelton, B. W.; White, A. H. *Aust. J. Chem.* **1997**, *50*, 539.

(23) Levason, W.; Matthews, M. L.; Reid, G.; Webster, M. *Dalton Trans.* **2004**, 554.

(24) Conradie, J.; Quarless, D. A.; Hsu, H.-F.; Harrop, T. C.; Lippard, S. J.; Koch, S. A.; Ghosh, A. *J. Am. Chem. Soc.* **2007**, *129*, 10446.

(25) Govindaswamy, N.; Quarless, D. A.; Koch, S. A. *J. Am. Chem. Soc.* **1995**, *117*, 8468.

(26) Pyykkö, P. *Chem. Rev.* **1997**, *97*, 597.

(27) Allen, F. *Acta Crystallogr., Sect. B* **2002**, *58*, 380.

(28) Willett, R. D.; Pon, G.; Nagy, C. *Inorg. Chem.* **2001**, *40*, 4342.

(29) Le Gall, B.; Conan, F.; Cosquer, N.; Kerbaol, J.-M.; Kubicki, M. M.; Vigier, E.; Le Mest, Y.; Sala Pala, J. *Inorg. Chim. Acta* **2001**, *324*, 300.

(30) Jagner, S.; Helgesson, G. *Adv. Inorg. Chem.* **1991**, *37*, 1.

(31) Hasselgren, C.; Stenhagen, G.; Öhrström, L.; Jagner, S. *Inorg. Chim. Acta* **1999**, *292*, 266.

(32) Levason, W.; Matthews, M. L.; Reid, G.; Webster, M. *Dalton Trans.* **2004**, 51.

(33) Sheldrick, G. M. *SHELXS-97, program for crystal structure solution*; University of Göttingen, Göttingen, Germany, 1997.

(34) Sheldrick, G. M., *SHELXL-97, program for crystal structure refinement*; University of Göttingen, Göttingen, Germany, 1997.